Solution and Crystal Structures of Chiral Molecules Can Be Significantly Different: *tert*-Butylphenylphosphinoselenoic Acid

Feng Wang and Prasad L. Polavarapu*

Department of Chemistry, Vanderbilt University, Nashville, Tennessee 37235

Józef Drabowicz, Piotr Kiełbasinski, Marek J. Potrzebowski, and Marian Mikołajczyk

Center of Molecular and Macromolecular Studies, Polish Academy of Sciences, 93-236 Łódż, Sienkiewicza 112, Poland

Michał W. Wieczorek

Institute of Chemistry and Environmental Protection, Pedagogical University of Częstochowa, Armii Krajowej 13/15, 42-200 Częstochowa, Poland

Wiesław W. Majzner and Izabella Łażewska

Institute of Technical Biochemistry, Technical University of Łódż Stefanowskiego 4/10, 90-924 Łódż, Poland

Received: November 25, 2003

In a majority of the cases, the structure of a molecule determined in the crystalline state is used to explain the properties of that molecule in the solution phase. To test the general applicability of such an approach, the structure of *tert*-butylphenylphosphinoselenoic acid has been determined both in the solution phase and in the crystalline state. To determine the structure in the solution phase, vibrational absorption and vibrational circular dichroism (VCD) spectra of the levorotatory enantiomer of *tert*-butylphenylphosphinoselenoic acid have been measured in $CDCl_3$ solution in the 2000−900 cm^{-1} region. The conformations for both tautomeric structures of monomeric (*S*)-*tert*-butylphenylphosphinoselenoic acid are investigated using the B3LYP functional with the 6-31G* basis set. Vibrational absorption and VCD spectra are predicted for these conformations at the same level. For the most stable conformation, the geometry, vibrational absorption, and VCD spectra are also predicted using the B3LYP functional with the aug-cc-pVDZ basis set. Similar investigations were also carried out for dimeric (*S*)-*tert*-butylphenylphosphinoselenoic acid. A comparison of the predicted spectra with corresponding experimental spectra in $CDCl_3$ solution indicates that (−)-*tert*-butylphenylphosphinoselenoic acid has the *S* configuration and exists predominantly as a monomer in one tautomeric structure and one conformation. The ab-initio-predicted specific rotation also confirms that (*S*)-*tert*-butylphenylphosphinoselenoic acid exists as a monomer in chloroform solution and that the absolute configuration is *S*-(−). The structure in the crystalline state has been determined using X-ray diffraction. Although the absolute configuration is fully supported by the X-ray structure, it is found that (*S*)-*tert*-butylphenylphosphinoselenoic acid exists in a crystal as an intermolecularly hydrogen-bonded dimer. This observation suggests that one should be careful in interpreting the solution-phase data using crystal structures.

Introduction

X-ray diffraction represents one of the most commonly used techniques to determine the structures of molecules whenever suitable crystals can be grown. These crystal structures are often used to interpret or generalize the properties of molecules in other environments, such as the solution phase. It is common knowledge that the crystal structures are often influenced by effects such as crystal packing and so forth, but there is no unique way of defining what the differences would be between structures in crystalline and solution phases. To establish such differences and generalize them if possible, it is necessary to determine the structures independently in both crystalline and solution phases for as many systems as possible. But such combined studies are hard to find in the literature. With the development of vibrational optical activity,[1] which comprises two independent techniques, namely, vibrational circular dichroism (VCD) and vibrational Raman optical activity (VROA), and specific rotation[2] as reliable techniques for determining the molecular structures in the solution phase, it is now possible to verify or establish any significant differences between the crystal and solution-phase structures. In this article, we present the structures determined in this manner for *tert*-butylphenylphosphinoselenoic acid in both solution and crystalline phases in order to assess the differences between these structures.

The characterization of phosphines has attracted much attention in recent years because they are extensively used in asymmetric and stereoselective synthesis.[3−5] In sharp contrast to this, the P-stereogenic phosphinic acid derivatives containing heavy atoms such as sulfur or selenium have been much less

* Corresponding author. E-mail: Prasad.L.Polavarapu@vanderbilt.edu. Fax: (615) 322-4936.

10.1021/jp031270h CCC: $27.50
Published on Web 02/20/2004

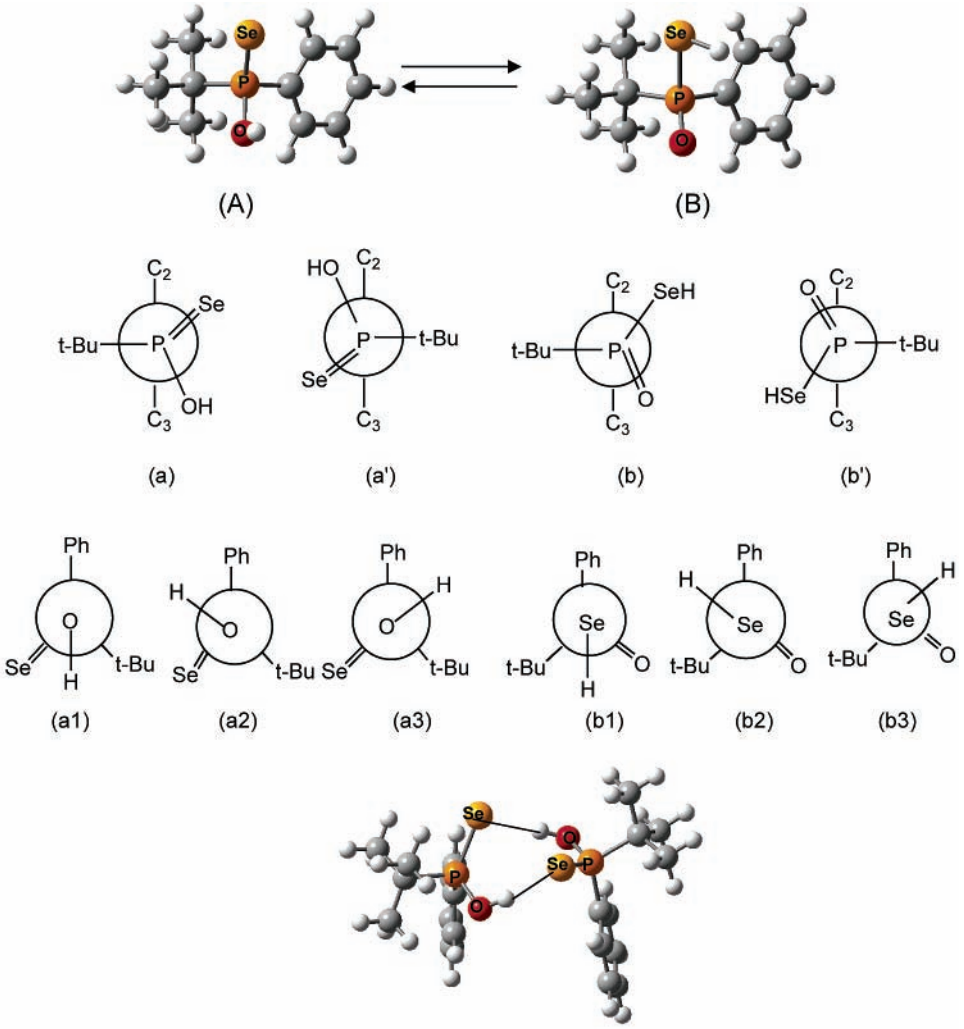

Figure 1. Tautomeric structures and different conformations of (*S*)-*tert*- butylphenylphosphinoselenoic acid (**1**). **A** and **B** are two tautomeric structures; **a** and **a**' are conformations around the C*t*−P−C_1−C_2 dihedral segment for **A**; **b** and **b**' are conformations around the C*t*−P−C_1−C_2 dihedral segment for **B**; **a1**, **a2**, and **a3** are conformations around the Se═P−O−H dihedral segment for **A**; and **b1**, **b2**, and **b3** are conformations around the O═P−Se−H dihedral segment for **B**. The bottom structure is that of the dimer, optimized at the B3LYP/6-31G* level, with the O−H···Se hydrogen bond depicted by a thin line.

studied although they can be considered to be useful stoichiometric and catalytic auxiliaries. For example, the enantiomeric *tert*-butylphenylphosphinothioic and *tert*-butylphenylphosphinoselenoic acids could be used as useful chiral solvating agents for the NMR determination of the enantiomeric excesses of a few optically active organic compounds with stereogenic carbon or heteroatoms.[6]

tert-Butylphenylphosphinoselenoic acid can be prepared by reacting *tert*-butylphenylphosphine oxide with elemental selenium and $(C_2H_5)_3N$ or by air oxidation of secondary *tert*-butylphenylphosphine selenide $(CH_3)_3C(C_6H_5)P(Se)H$, and it was resolved into its enantiomers via the salts with (+)−(C_6H_5)-$CH(CH_3)NH_2$.[7] (−)-*tert*-Butylphenylphosphine oxide was earlier assigned to the *S* configuration by chemical correlation,[8] and this assignment was recently confirmed using vibrational circular dichroism (VCD).[9] Upon deselenization, (+)-*tert*-butylphenylphosphinoselenoic acid gave (−)-*tert*-butylphenylphosphine oxide, and on the basis of this observation, (+)-*tert*-butylphenylphosphinoselenoic acid was assigned to the *R* configuration.[8a] Analogously, (+)-*tert*-butylphenylphosphinothioic acid was assigned to the *R* configuration by chemical correlation,[8a] and this assignment has been confirmed by VCD spectroscopy.[10] The absolute configuration of *tert*-butylphenylphosphinoselenoic acid, however, has not yet been confirmed by an independent spectroscopic method. It should be noted that *tert*-butylphenylphosphinoselenoic acid, like secondary phosphine oxides, phosphites, and phosphorothioates,[11] can exist in equilibrium between different tautomeric structures **A** and **B** (Figure 1). Neither the stability of different tautomeric forms nor the predominant conformation of *tert*-butylphenylphosphinoselenoic acid has been established.

Vibrational circular dichroism (VCD) is an independent spectroscopic method that has become a reliable tool for the determination of the absolute configuration and predominant conformations of chiral molecules.[12] In addition, the combination of ab initio and experimental vibrational spectroscopic methods can be used to study chemical reactions and elucidate their equilibrium.[13] Ab initio predictions of specific rotation have also emerged in the past few years as an alternate, independent, reliable method for determining the molecular structure.[2,14] Here one predicts the specific rotation for a given configuration with all plausible conformations at an appropriate ab initio theoretical level and compares the sign and magnitude of the predicted values with those of the corresponding experimental value to establish the structure.

The equilibrium between tautomeric structures and their dominant conformations has been determined for *tert*-butylphenylphosphine oxide and *tert*-butylphenylphosphinothioic acid

using theoretical and experimental VCD spectra[9,10] and specific rotation.[14] Such information is not available for *tert*-butylphenylphosphinoselenoic acid. Here we report the VCD and specific rotation studies on (−)-*tert*-butylphenylphosphinoselenoic acid using state-of-the-art experimental and theoretical predictions with the density functional method and different basis sets. From a comparison of theoretical and experimental data, the structure of chiral *tert*-butylphenylphosphinoselenoic acid in the solution phase is elucidated. The structure of (−)-*tert*-butylphenylphosphinoselenoic acid in the crystalline phase is obtained from X-ray diffraction studies. It is found that whereas all three methods used are in agreement with regard to the absolute configuration there are significant differences among the structures deduced in solution and the crystalline phase.

Experimental Methods

General. NMR spectra were recorded at 200 MHz. Polarimetric measurements were made on a Perkin-Elmer 241M photopolarimeter.

Racemic and Enantiomeric *tert*-Butylphenylphosphinoselenoic Acid. Racemic *tert*-butylphenylphosphinoselenoic acid was prepared by the addition of elemental selenium to racemic *tert*-butylphenylphosphine oxide in the presence of triethylamine.[7] The crude triethylammonium salt of the acid formed was converted to the free acid via acidification of its aqueous solution with dilute hydrochloric acid. The acid formed was extracted with chloroform, and the solution was dried with anhydrous magnesium sulfate. After the evaporation of the solvent, pure *tert*-butylphenylphosphinoselenoic acid was obtained. ^{1}H NMR ($CDCl_3$) δ: 1.15 (d, $J = 18.1$ Hz, 9H), 7.27−7.47 (m, 3H), 7.35−7.83 (m, 2H). ^{31}P NMR ($CDCl_3$) δ: 97.8 (sidebands $J_{P31-Se77} = 739$ Hz). Enantiomers of *tert*-butylphenylphosphinoselenoic acid were isolated via its diastereomeric salts with each enantiomer of α-methylbenzylamine. Particular enantiomers were liberated from the corresponding salts by acidification with hydrochloric acid[10] and exhibited the following optical rotations: the dextrorotatory enantiomer $[\alpha]_D = +51$ ($c = 1.77$, $CHCl_3$); the levorotatory enantiomer $[\alpha]_D = -50.2$ ($c = 2.06$, $CHCl_3$). The spectral data (^{1}H and ^{31}P NMR) were identical to those recorded for racemic *tert*-butylphenylphosphinoselenoic acid.

Measurements. The infrared and VCD spectra were recorded on a commercial Fourier transform VCD spectrometer. The VCD spectra were recorded for 3 h at 4-cm^{-1} resolution. Spectra were measured in $CDCl_3$ solvent at 0.172 M and at a path length of 200 μm. Spectra for (−)-*tert*-butylphenylphosphinoselenoic acid have also been collected in $CDCl_3$ solvent at 0.086 and 0.043 M. The sample was held in a variable-path-length cell with BaF_2 windows. In the presented absorption spectra, the solvent absorption was subtracted. In the presented VCD spectra, the raw VCD spectrum of the solvent was subtracted.

Calculations. The ab initio vibrational frequencies, absorption, and VCD intensities for (*S*)-butylphenylphosphinoselenoic acid were calculated using the Gaussian 98 program.[15] The calculations used density functional theory with a Becke-style[16] B3LYP hybrid functional and 6-31G*, 6-311G (2d,2p), and aug-cc-pVDZ basis sets.[13] The B3PW91 functional and 6-31G* and 6-311G (2d,2p) basis sets were also used in calculations, but the results were not improved. The procedure for calculating the VCD intensities using DFT theory is due to Cheeseman et al.[17] as implemented in the Gaussian 98 program.[15] The theoretical absorption and VCD spectra were simulated with Lorentzian band shapes and a 5-cm^{-1} full width at half-height. Because the ab initio-predicted band positions are higher than the experimental values, the ab initio frequencies obtained with the 6-31G* basis set were scaled by 0.9613. Specific rotations at the DFT and HF levels were calculated using linear response theory and gauge including atomic orbitals as implemented in the DALTON program.[18]

Crystal and Molecular Structures of the Levorotatory Enantiomer of *tert*-Butylphenylphosphinoselenoic Acid. The crystal and molecular structures of (−)-(*S*)-*tert*-butylphenylphosphinoselenoic acid were determined using data collected at room temperature on a CAD4 diffractometer with graphite-monochromatized Cu Kα radiation. The compound crystallizes in the orthorhombic system, in space group $P2_12_12_1$ with the unit cell consisting of eight molecules. The lattice constants were refined by a least-squares fit of 25 reflections in the θ range of 18.98−30.49°. The decline in the intensities of three control reflections (3, −3, −2; −1, −4, −7; −2, −5, 1) was 43.8% during 80.2 h of exposure time. An empirical absorption correction was applied by the use of the ψ-scan method (EAC program).[19,20]

A total of 4184 observed reflections with $I \geq 0\sigma(I)$ were used to solve the structure by direct methods and to refine it by full matrix least-squares[21,22] using F^2. Hydrogen atoms for hydroxyl groups were found on a difference Fourier map. Hydrogens attached to carbon atoms were placed geometrically at idealized positions and set as riding with the C−H distance free to refine; for methylene groups, the rotation about the C−C bond was also allowed. Anisotropic thermal parameters were refined for all non-hydrogen atoms; all H atoms were refined isotropically.

The final refinement converged to $R = 0.0391$ for 293 refined parameters and 3489 observed reflections with $I \geq 2\sigma(I)$. The absolute configuration at the chiral atom was established as S_{P3}. The absolute structure was determined by the Flack method[23] with the result $\chi = -0.01(4)$. Data corrections were carried out with the Enraf-Nonius SDP crystallographic computing package,[19] the structure solution SHELXS,[21] and the structural refinement SHELXL.[22]

We have deposited all crystallographic data for this structure in the Cambridge Crystallographic Data Centre.[24]

Results and Discussion

Vibrational Circular Dichroism Studies. The geometries were optimized at the B3LYP/6-31G* level using standard dihedral angles of 0, 60, 120, 180, 240, or 300° for the C*t*−P−C_1−C_2 segment (where C*t* is the central carbon atom of the *tert*-butyl group, see Figure 1) for the two tautomeric structures of (*S*)-*tert*-butylphenylphosphinoselenoic acid. These starting geometries converged to two conformations for each of the two tautomeric forms, differing in dihedral angles for C*t*−P−C_1−C_2 segment (**a** and **a′** for tautomeric structure **A**; **b** and **b′** for tautomeric structure **B**) as shown in Figure 1. However, because of the symmetry of the benzene ring, the two conformations based on the dihedral angle C*t*−P−C_1−C_2 for each tautomeric structure have the same energies, and they cannot be distinguished. Keeping the C*t*−P−C_1−C_2 segment in the gauche plus (labeled **a** and **b**) conformation, the stability of the resulting three conformations based on the difference in the dihedral angles H−O−P═Se and H−Se−P═O of forms **A** and **B** was studied (**a1**, **a2**, **a3**, **b1**, **b2**, and **b3** in Figure 1). Only one stable conformation **a2** is obtained for tautomeric structure **a**; **a1** and **a3** conformations converged to **a2** (possibly because of the interaction between the hydroxyl hydrogen atom and the benzene ring and selenium). For tautomeric structure **B**, three stable conformations are obtained. The converged dihedral angles, optimized electronic energies, Gibbs energies, and relative populations are listed in Table 1. Tautomeric form **A**

TABLE 1: Conformations and B3LYP/6-31G* Energies of Monomeric (*S*)-*tert*-Butylphenylphosphinoselenoic Acid

label[a]	dihedral angles[b] D_1	D_2	D_3	D_4	energy[c] electronic	Gibbs	ΔE[d] (kcal/mol)	pop.[e] (%)
a2 gt	102.0	−26.5	−151.3	−18.4	−3206.112484	−3205.922812	0	97.6
b3 gg-	88.2	−18.4	−145.7	49.7	−3206.105601	−3205.919050	2.4	1.9
b1 gt	72.4	−38.8	−162.7	−56.1	−3206.103462	−3205.917785	3.1	0.5
b2 gg	99.5	−14.0	−135.0	−160.0	−3206.100941	−3205.913916	5.6	0

[a] See Figure 1 for the labels. [b] Dihedral angles are in degrees. D_1 stands for C*t*−P−C_1−C_2; D_2, for C_2−C_1−P−Se; and D_3, for C_2−C_1−P−O. D_4 stands for Se−P−O−H for tautomeric form **A**, and O−P−Se−H stands for tautomeric form **B**. [c] In hartrees. [d] Relative energy difference in kcal/mol. [e] Population percentage based on Gibbs energies.

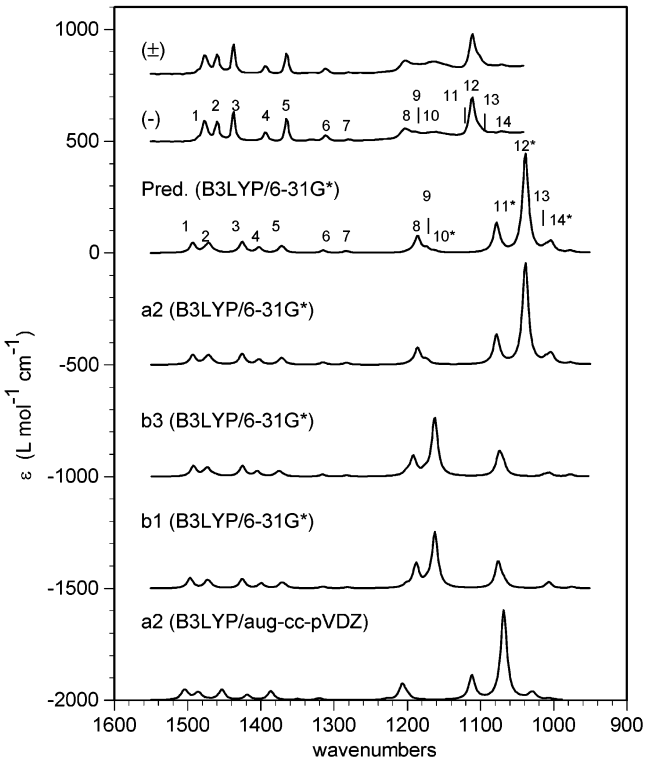

Figure 2. Comparison of the experimental absorption spectra of enantiomeric *tert*- butylphenylphosphinoselenoic acid at ∼0.17 M in $CDCl_3$ solution (top two traces) with the predicted absorption spectra (bottom four traces) of stable conformations of the *S* configuration (structure and conformation labels in Figure 1) obtained with different basis sets. The trace labeled "Pred" (third from top) is the population-weighted spectrum, with populations given in Table 1. Bands 10−12 and 14, marked with astreisks, are expected to be influenced by intermolecular hydrogen bonding in solution.

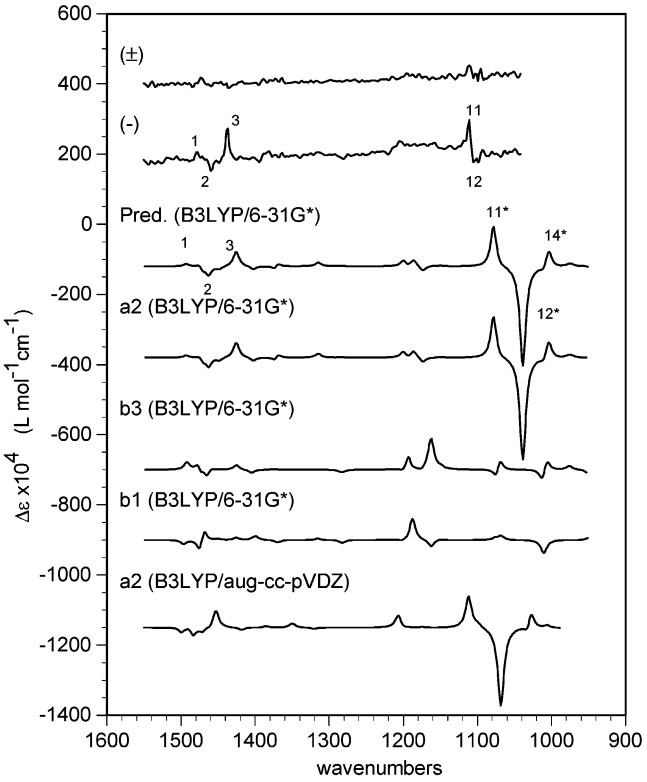

Figure 3. Comparison of the experimental VCD spectra of enantiomeric *tert*- butylphenylphosphinoselenoic acid at ∼0.17 M in $CDCl_3$ solution (top two traces) with the predicted VCD spectra (bottom four traces) of stable conformations of the *S* configuration (structure and conformation labels in Figure 1) obtained with different basis sets. The trace labeled "Pred" (third from top) is the population-weighted spectrum, with populations given in Table 1. Bands 10−12 and 14, marked with asterisks, are expected to be influenced by intermolecular hydrogen bonding in solution.

has a much lower energy than tautomeric form **B**. On the basis of the relative populations, the equilibrium constant is predicted to be ∼0.025 for the equilibrium between two tautomeric structures of *tert*-butylphenylphosphinoselenoic acid. Thus, for isolated monomeric (*S*)-*tert*-butylphenylphosphinoselenoic acid, the predominant tautomeric structure is **A**, and the conformation is **a2**.

The converged tautomeric forms were found to have potential energy minima (i.e., all vibrational frequencies are real) at the B3LYP/6-31G* level. The absorption and VCD intensities were calculated for **a2**, **b3**, and **b1** conformations at the B3LYP/6-31G* level. The predicted absorption and VCD spectra were simulated with 5-cm^{-1} half widths and Lorentzian band shapes. The theoretical spectra for the predominant conformation **a2** can be compared to the experimental spectra in Figures 2 and 3.

The experimental absorption spectra obtained for 0.17 M $CDCl_3$ solution are shown in Figure 2, where the absorption spectrum of the solvent has been subtracted. The absorption bands in the predicted spectrum (B3LYP/6-31G*) for conformation **a2** show a one-to-one correspondence with the absorption bands in the experimental spectrum, but the following differences are to be noted. (a) The predicted relative intensities of the bands for conformation **a2** in the range from 1100 to 900 cm^{-1} are much larger than those of the corresponding bands in the experimental spectra, and the band positions in the predicted spectrum are much lower than those in the experimental spectra in this region. (b) The relative intensity of the band at 1166 cm^{-1} (no. 10) in the experimental spectrum is much larger than that in the predicted spectrum. (c) The bands at 1078 (no. 11) and 1039 (no. 12) cm^{-1} in the predicted spectrum are more separated from each other than those in the experimental spectrum. Except for these differences, the experimental spectra in $CDCl_3$ solution are considered to be in reasonable agreement with the predicted absorption spectrum for conformation **a2**. On the basis of vibrational assignments, some bands in the region from 1200 to 900 cm^{-1} (marked with asterisks in Table

TABLE 2: Comparison of Predicted Frequencies for Monomeric *tert*- Butylphenylphosphinoselenoic Acid with the Observed Frequencies and Vibrational Assignments

label[a]	exptl[b] (cm^{-1})	calcd[c,f] (cm^{-1})	pred[d,e] (cm^{-1})	calcd[d,f] (cm^{-1})	assignments[g]
1	1476.6	1504.9	1493.0	1553.1	CH3 def
2	1459.5	1488.2	1471.6	1530.8	CH3 def, CH bending
3	1437.6	1453.3	1425.6	1483.0	ring def., CH bending
4	1493.5	1418.7	1402.8	1459.3	CH3 def.
5	1364.5	1387.2	1371.7	1426.9	CH3 def.
6	1311.3	1349.9	1314.8	1367.7	ring def., CH bending
7	1279.9	1320.6	1283.4	1335.1	ring def., CH bending
8	1214.5	1206.9	1185.9	1233.7	CH3 wag, C−P stretching
9	1188.9	1200.2	1175.3	1222.6	ring C−H bending
10*	1166.3		1162.6	1209.4	P═O and P−C stretching, CH3 wag
11*	1117.2	1111.8	1078.2	1121.6	P−C stretching, POH bending, and ring def.
12*	1111.2	1068.2	1038.7	1080.5	POH bending, CH3 wag.
13	1100.5	1031.8	1010.7	1051.4	CH3 wag
14*	1072.6	1027.7	1004.2	1044.6	CH3 wag, POH bending

[a] These numbers are derived from those in Figure 2; asterisks denote bands that are expected to be influenced by the formation of intermolecular hydrogen bonds. [b] Experimental wavenumbers obtained from the absorption spectrum at a concentration of ∼0.17 M. [c] Band positions from the simulated spectra of conformation **a2** based on the B3LYP/aug-cc-pVDZ calculation given in Figure 2. Band 10 is not listed because the B3LYP/aug-cc-pVDZ calculation was not done for conformer **b3**. [d] Band positions from the simulated spectra based on B3LYP/6-31G* calculations given in Figure 2. [e] Ab initio wavenumbers scaled with 0.96. [f] Unscaled ab initio wavenumbers. [g] Deduced from GaussView (version 2.1) based on the B3LYP/6-31G* calculations.

2 and Figures 2 and 3) are attributed to P═O stretching (from conformations **b3** and **b1**) or POH bending vibrations (from conformation **a2**). The formation of intermolecular hydrogen bonds could make these bands shift to higher frequencies in the solution phase. The differences between experimental and theoretical frequencies can arise from such hydrogen bonding effects in the experimental data or from the inadequacy of the basis set used (vide infra).

The experimental VCD spectra obtained for 0.17 M $CDCl_3$ solution are shown in Figure 3, where the VCD spectrum of the solvent has been subtracted. The significant VCD bands in the experimental VCD spectrum of (−)-*tert*-butylphenylphosphinoselenoic acid are a positive−negative−positive triplet with a positive maximum at 1477 (no. 1) cm^{-1}, a negative maximum at 1460 (no. 2) cm^{-1}, a positive band at 1438 (no. 3) cm^{-1}, and positive−negative couplets at 1117 (no. 11) and 1111 (no. 12) cm^{-1}. The same features are seen in the predicted VCD spectrum for the (*S*)-*tert*-butylphenylphosphinoselenoic acid except that (a) the bands in 1100−900 cm^{-1} region are more prominent in the predicted VCD spectrum, (b) bands at 1117 (no. 11) and 1111 (no. 12) cm^{-1} are closer to each other in the experimental VCD spectrum, and (c) the positive band corresponding to the predicted positive band at 1004 cm^{-1} (no. 14) is not evident in the experimental VCD spectrum. These observations point to the influence of possible hydrogen bonding effects in the experimental spectra or to the inadequacy of the basis set used in the calculations.

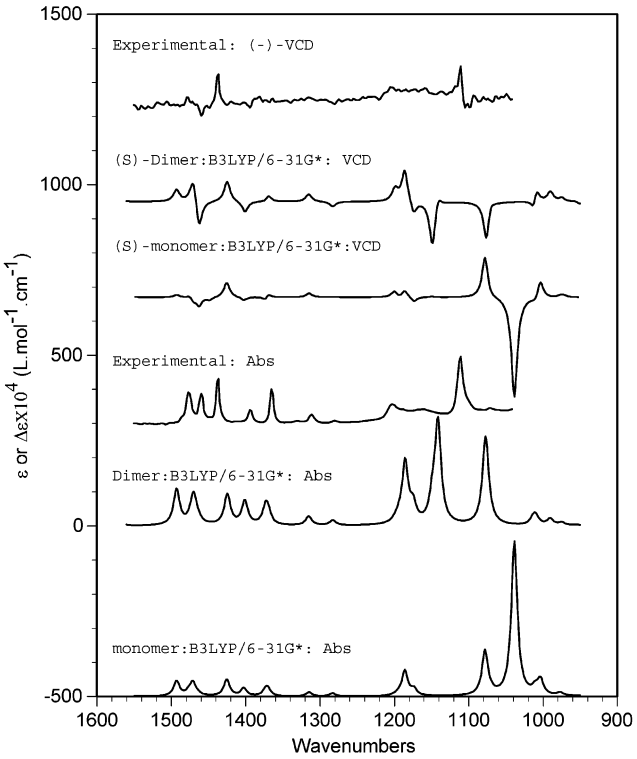

Figure 4. Comparison of the experimental absorption and VCD spectra of (−)-*tert*-butylphenylphosphinoselenoic acid at ∼0.17 M in $CDCl_3$ solution with the predicted spectra for the monomeric **a2** conformation and dimer, both with the *S* configuration (structure and conformation shown in Figure 1), obtained with the B3LYP/6-31G* basis set.

To consider the influence of intermolecular hydrogen bonding and the resulting dimers, investigations were also undertaken on the dimeric form of (S)-*tert*-butylphenylphosphinoselenoic acid (Figure 1). The geometry of the dimer was fully optimized at the B3LYP/6-31G* level. The O−H···Se distance in the optimized structure of the isolated dimer is 2.302 Å. Vibrational absorption and VCD spectra were calculated at this optimized geometry using B3LYP/6-31G* theory. These spectra are compared to the experimental spectra and predicted monomer spectra in Figure 4. For the isolated dimer, B3LYP/6-31G* calculations predict a Gibbs energy of −6411.858986 hartrees, which translates to −3205.929493 hartrees/monomer unit and is lower than the monomer energies listed in Table 1. Thus, the dimer is energetically favored over the monomer in vacuum. However, these calculations did not include the solvent influence, so the situation in $CDCl_3$ solution can be different. From the comparison of predicted and experimental spectra, shown in Figure 4, it can be seen that the predicted dimer spectra differ significantly from the experimental spectra. In the predicted absorption spectrum for the dimer, there are three strong absorption bands in the 1250−1050-cm^{-1} region. The experimental absorption spectrum in the same region shows only one strong band at 1111 cm^{-1}. As a result, it is unlikely that dimers are dominant in $CDCl_3$ solution at the concentrations used.

The positions and intensities of the bands in the B3LYP/6-31G* predicted absorption and VCD spectra of conformation **b3** do not match those experimentally observed (Figures 2 and 3). However, the larger relative intensity observed at 1166 cm^{-1} (no. 10) in the experimental absorption spectrum suggests that either tautomeric structure **B** or the dimer or both are probably present in solution (more than that predicted for isolated molecule; see Table 1) because this band can be attributed to conformations **b3** or **b1** or the dimer (Figures 2 and 4). From

the absorption spectra collected at different concentrations (0.043−0.172 M), we note that the relative intensity of this band decreases as the concentration increases. No other obvious changes have been observed with changes in concentration. In the structure of conformation **a2**, the Se, P, O, and H atoms are almost in the same plane, suggesting that the interaction between Se and H atoms is significant. At dilute concentrations, the interaction between Se and H atoms may favor the formation of tautomeric structure **B**, whose presence is indicated by the presence of band 10 in the experimental absorption spectrum. At higher concentrations, the intermolecular hydrogen bonding influence appears to favor tautomeric structure **A** (as evidenced by the decrease in absorption intensity of band 10 at higher concentrations). Although tautomeric structure **B** appears to be more populated than that predicted for isolated molecule (Table 1), tautomeric structure **A** is still the most predominant one in $CDCl_3$ solution.

The discussion presented above for predicted spectra pertains to those obtained at the B3LYP/6-31G* level. To investigate the influence of the basis set on the observed differences between experimental and predicted spectra, calculations for conformation **a2** were also undertaken with larger basis sets, 6-311G(2d,2p) and aug-cc-pVDZ, using the same functional. The B3PW91 functional was also used in the calculations. The geometry of the **a2** conformation was optimized with these basis sets, and vibrational absorption and VCD spectra were obtained at the optimized geometry. However, except for the calculations using B3LYP/aug-cc-pVDZ, the results from other calculations are not significantly different from those of B3LYP/6-31G* calculations. The results obtained from the B3LYP/aug-cc-pVDZ calculation are presented, along with B3LYP/6-31G* results, in Figures 2 and 3. As can be seen in Figures 2 and 3, the band positions obtained in the B3LYP/aug-cc-pVDZ calculation are in better agreement with experimental band positions, but the overall spectral pattern did not change significantly in this calculation. It appears that the B3LYP/aug-cc-pVDZ calculation provides a better prediction of experimental vibrational band positions.

It is somewhat unusual that the difference between observed and B3LYP/6-31G* calculated frequencies is rather large in the 1100−900-cm^{-1} region for this molecule. The same observation was also noted for *tert*-butylphenylphosphinothioic acid.[10] Thus, it appears that for phosphorus compounds that contain heavy atoms it is necessary to use very large basis sets, such as aug-cc-pVDZ, to achieve better agreement between calculated and observed vibrational band positions.

Because the VCD sign pattern predicted for the monomeric **a2** conformation of (*S*)-*tert*-butylphenylphosphinoselenoic acid matches that observed for (−)-*tert*-butylphenylphosphinoselenoic acid, these results indicate that (−)-*tert*-butylphenylphosphinoselenoic acid exists as a monomer in dilute $CDCl_3$ solutions and that its absolute configuration can be assigned as (*S*)-(−).

Specific Rotation Studies. To analyze the structure of *tert*-butylphenylphosphinoselenoic acid further, the specific rotation $[\alpha]_D$ was predicted ab initio and compared to the experimental rotation (Table 3). Using the B3LYP/6-31G* optimized structure for the **a2** conformation of monomeric (*S*)-*tert*-butylphenylphosphinoselenoic acid, the $[\alpha]_D$ values predicted at the HF/6-31G*, B3LYP/6-31G*, and B3LYP/6-311++G(2d,2p) levels are, respectively, −56, −84, and −70. The specific rotation predicted for dimeric (*S*)-*tert*-butylphenylphosphinoselenoic acid, using the B3LYP/6-31G*-optimized geometry of the dimer, is −287 at the HF/6-31G* level and −415 at the B3LYP/6-31G* level.

TABLE 3: Comparison of the Specific Rotation Predicted for (*S*)-*tert*-Butylphenylphosphinoselenoic Acid with the Observed Specific Rotation

	HF/6-31G*	B3LYP/6-31G*	B3LYP/ 6-311++G(2d,2p)[a]	exptl
monomer	−56	−84	−70	−50
dimer	−287	−415		

[a] The calculation for the dimer at this level could not be undertaken because of the large number of basis functions involved.

TABLE 4: Crystal Data and Experimental Details

molecular formula	$C_{10}H_{15}OPSe$
formula weight	261.15
crystallographic system	orthorhombic
space group	$P2_12_12_1$
a (Å)	6.5958(6)
b (Å)	17.225(3)
c (Å)	21.182(4)
V (Å^3)	2406.6(6)
Z	8
D_c (g/cm^3)	1.442
μ [mm^{-1}]	5.183
crystal dimensions (mm)	0.15 × 0.20 × 0.6
maximum 2θ (°)	139.96
radiation, λ (Å)	Cu Kα, 1.54184
scan mode	$\omega/2\theta$
scan width (deg)	$0.75 + 0.14 \tan\theta$
hkl ranges:	$h = 0-8$
	$k = -21-0$
	$l = -26-26$
EAC correction:	min. 0.8129
	max. 0.9997
	ave. 0.9273
DECAY correction:	min. 1.00019
	max. 1.33404
	ave. 1.14343
no. of reflections:	unique 4551
	with $I > 0\sigma(I)$ 4184
	obsd with $I > 2\sigma(I)$ 3489
no. of parameters refined	293
largest diff. peak (e Å^{-3})	0.389
largest diff. hole (e Å^{-3})	−0.448
shift/esd max	0.001
R_{obs}	0.0391
wR_{obs}	0.0937
S_{obs}	1.096
weighting coeff[a]:	m 0.0549
	n 0.0000
R_{int}	0.0275
T_{meas}	293(2)
$F(000)$	1056
absolute structure	S_{P1}
flack parameter χ	−0.01(4)

[a] Weighting scheme $w = [\sigma^2(F_o^2) + (mP)^2 + nP]^{-1}$ where $P = (Fo^2 + 2Fc^2)$.

The observed specific rotation in chloroform solution is −50. These data indicate that the magnitude of the predicted specific rotation for dimeric (*S*)-*tert*-butylphenylphosphinoselenoic acid deviates significantly from the experimental specific rotation. The predicted specific rotation for the monomeric **a2** conformation of (*S*)-*tert*-butylphenylphosphinoselenoic acid is in close agreement with the experimentally observed specific rotation. Thus, specific rotation studies support the conclusions derived from VCD studies that in chloroform solution (*S*)-*tert*-butylphenylphosphinoselenoic acid exists predominantly in its monomeric form and its absolute configuration is (*S*)-(−).

Crystal and Molecular Structures of (−)-*tert*-Butylphenylphosphinoselenoic Acid. Crystal data are given in Table 4. The X-ray crystal structure determination, which was carried out on a single crystal of the levorotatory enantiomer by

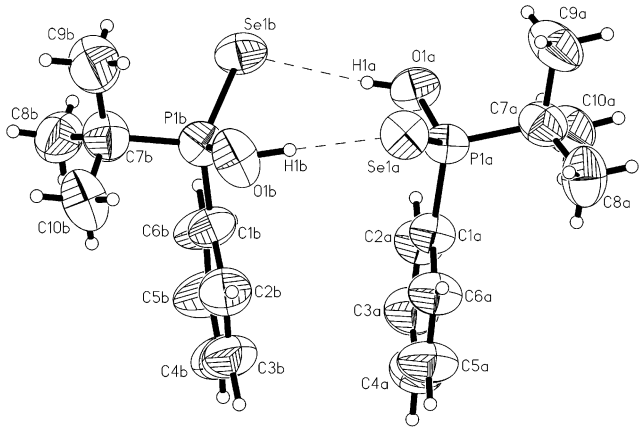

Figure 5. Thermal ellipsoidal view with the atom numbering scheme of the (−)-(*S*)-*tert*-butylphenylphosphinoselenoic acid molecules. Ellipsoids are shown with 50% probability.

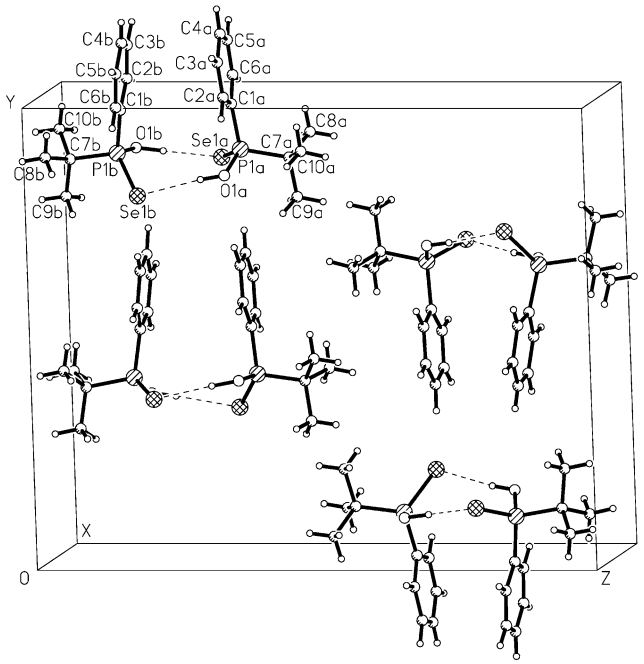

Figure 6. Crystal-packing diagram of (−)-(*S*)-*tert*-butylphenylphosphinoselenoic acid.

anomalous dispersion, unequivocally revealed that the absolute configuration at the stereogenic phosphorus atom in (−)-**1** is *S*, which is clearly shown in Figure 5. The unit cell of **1** consists of eight molecules that form in the crystal lattice four pairs of dimers stabilized by the intramolecular hydrogen bonds via the $O1_a-H1_a\cdots Se1_b$ and $O1_b-H1_b\cdots Se1_a$ interactions (Figure 6). The O−H·····Se distances are equal to 2.33(12) Å. The absolute configuration deduced from X-ray studies confirms that deduced from VCD and specific rotation studies. However, it should be noted that in the crystal structure the molecules are packed as dimers whereas in solution there is no evidence of the predominance of dimers. It is also of interest that in the crystal structure of the dimer (Figures 5 and 6) the phenyl rings point inward (toward each other) from the perfect parallel orientation by an angle of 10.68 °; when viewed along the P···P connecting line, the two phenyl rings are seen to be nearly eclipsed. (The $C_{ph}-P\cdots P-C_{ph}$ dihedral angle, where C_{ph} is the phenyl carbon atom attached to phosphorus, is −9 °, the P···P distance is 4.54 Å, and the $C_{ph}\cdots C_{ph}$ distance is 4.10 Å.) In the structure of the isolated dimer (Figure 1), the phenyl rings point outward from a perfect parallel orientation, and when viewed along the P···P connecting line, the two phenyl rings are seen to be staggered. (The $C_{ph}-P\cdots P-C_{ph}$ dihedral angle is $\sim -46°$, the P···P distance is 4.56 Å, and the $C_{ph}\cdots C_{ph}$ distance is 5.08 Å.) These differences between isolated and crystalline dimer structural parameters point to significant packing effects in the crystalline state.

Conclusions

All three methods used, namely, VCD, specific rotation, and X-ray diffraction, conclude independently that (−)-*tert*-butylphenylphosphinoselenoic acid is of the *S* configuration. The assignment of absolute configuration is in agreement with the literature.[8a] Tautomeric structure **A** with conformation **a2** is dominant for (−)-*tert*-butylphenylphosphinoselenoic acid in $CDCl_3$ solution. Evidence for a minor proportion of tautomeric structure **B** in $CDCl_3$ solution is present in the absorption spectra, but there is no evidence of the predominance of dimers in solution. This is in contrast to the solid-state structure, where X-ray diffraction data clearly show the presence of dimers. The structure of the isolated dimer, as predicted by the B3LYP/6-31G* calculation, is significantly different from that in the crystalline state, reflecting the dominance of packing effects over $\pi-\pi$ interactions between the phenyl groups. These differences underline the importance of determining both solution- and crystalline-phase structures of a given molecule independently.

Acknowledgment. We thank Dr. K. Ruud for providing a developmental version of the DALTON program, which was used to calculate the specific rotations reported here. This material is based upon work supported by the National Science Foundation under grant no. 0092922. Studies in Lodz were partially supported by the State Committee for Scientific Research under grant no. 4T09A10622. Any opinions, findings, and conclusions or recommendations expressed in this material are those of the authors and do not necessarily reflect the views of the National Science Foundation.

Supporting Information Available: Cartesian coordinates for the three tautomeric structures of monomeric (*S*)-*tert*-butylphenylphosphinoselenoic acid and dimeric (*S*)-*tert*-butylphenylphosphinoselenoic acid, optimized at the B3LYP/6-31G* level. Fractional atomic coordinates, anisotropic displacements of non-hydrogen atoms, bond lengths, and distances of atoms from phenyl ring planes obtained from X-ray crystallographic data. This material is available free of charge via the Internet at http://pubs.acs.org.

References and Notes

(1) (a) Barron, L. D. *Molecular Light Scattering and Optical Activity*; Cambridge University Press: 1982. (b) Diem, M. *Introduction to Vibrational Spectroscopy*; Wiley & Sons: New York, 1993. (c) Polavarapu, P. L. *Vibrational Spectra: Principles and Applications with Emphasis on Optical Activity*; Elsevier: New York, 1998.

(2) Polavarapu, P. L. *Mol. Phys.* **1997**, *91*, 551−554.

(3) Pietrusiewicz, K. M.; Zabłocka, M. *Chem. Rev.* **1994**, *9*, 1375.

(4) (a) Noyori, R. *Asymmetric Catalysis in Organic Synthesis*; Wiley & Sons: New York, 1994. (b) Quin, L. D. *A Guide to Organophosphorus Chemistry*; Wiley-Interscience: New York, 2000. (c) *Catalytic Asymmetric Synthesis*; Ojima, I., Ed.; Wiley-VCH: New York, 2000.

(5) Drabowicz, J.; Łyżwa, P.; Omelańczuk, J.; Pietrusiewicz, K. M.; Mikołajczyk, M. *Tetrahedron: Asymmetry* **1999**, *10*, 2757.

(6) For recent applications of enantiomeric *tert*-butylphenylphosphinothioic acid, see Mikołajczyk, M.; Mikina, M.; Jankowiak, A. *J. Org. Chem.* **2000**, *65*, 5127−5130. Mikołajczyk, M.; Łuczak, J.; Kiełbasiński, P. *J. Org. Chem.* **2002**, *67*, 7872−7875.

(7) Krawiecka, B.; Skrzypczyński, Z.; Michalski, J. *Phosphorus* **1973**, *3*, 177.

(8) (a) Michalski, J.; Skrzypczyński, Z. *J. Organomet. Chem.* **1975**, *97*, C31−C32. (b) Skrzypczyński, Z.; Michalski, J. *J. Org. Chem.* **1988**, *53*, 4549. (c) Haynes, R. K.; Freeman, R. N.; Mitchell, C. R.; Vonwiller, S. C. *J. Org. Chem.* **1994**, *59*, 2919.

(9) Wang, F.; Polavarapu, P. L.; Drabowicz, J.; Mikołajczyk, M. *J. Org. Chem*. **2000**, *65*, 7561−7565.

(10) Wang, F.; Polavarapu, P. L.; Drabowicz, J.; Mikołajczyk, M.; Łyżwa, P. *J. Org. Chem*. **2001**, *66*, 9015.

(11) Stawiński, J. *Handbook of Organophosphorus Chemistry*; Engel, R., Ed.; Marcel Dekker: New York, 1992; p 377.

(12) (a) Wang, F.; Wang, Y.; Polavarapu, P. L.; Li, T.; Drabowicz, J.; Pietrusiewicz, K. M.; Zygo, K. *J. Org. Chem*. **2002**, *67*, 6539. (b) Freedman, T. B.; Dukor, R. K.; van Hoof, P. J. C. M.; Kellenbach, E. R.; Nafie, L. A. *Helv. Chim. Acta* **2002**, *85*, 1160. (c) Devlin, F. J.; Stephens, P. J.; Scafato, P.; Superchi, S.; Rosini, C. *Chirality* **2002**, *14*, 400. Ashvar, C. S.; Stephens, P. J.; Eggimann, T.; Wieser, H. *Tetrahedron: Asymmetry* **1998**, *9*, 1107.

(13) Hehre, W. J.; Radom, L.; Schleyer, P. V. R.; Pople, J. A. *Ab initio Molecular Orbital Theory*; Wiley & Sons: New York, 1986.

(14) For a recent review, see Polavarapu, P. L. *Chirality* **2002**, *14*, 768. Polavarapu, P. L. *Chirality* **2002**, *15*, 284.

(15) Frisch, M. J.; Trucks, G. W.; Schlegel, H. B.; Scuseria, G. E.; Robb, M. A.; Cheeseman, J. R.; Zakrzewski, V. G.; Montgomery, J. A., Jr.; Stratmann, R. E.; Burant, J. C.; Dapprich, S.; Millam, J. M.; Daniels, A. D.; Kudin, K. N.; Strain, M. C.; Farkas, O.; Tomasi, J.; Barone, V.; Cossi, M.; Cammi, R.; Mennucci, B.; Pomelli, C.; Adamo, C.; Clifford, S.; Ochterski, J.; Petersson, G. A.; Ayala, P. Y.; Cui, Q.; Morokuma, K.; Malick, D. K.; Rabuck, A. D.; Raghavachari, K.; Foresman, J. B.; Cioslowski, J.; Ortiz, J. V.; Stefanov, B. B.; Liu, G.; Liashenko, A.; Piskorz, P.; Komaromi, I.; Gomperts, R.; Martin, R. L.; Fox, D. J.; Keith, T.; Al-Laham, M. A.; Peng, C. Y.; Nanayakkara, A.; Gonzalez, C.; Challacombe, M.; Gill, P. M. W.; Johnson, B. G.; Chen, W.; Wong, M. W.; Andres, J. L.; Head-Gordon, M.; Replogle, E. S.; Pople, J. A. *Gaussian 98*, revision A.3; Gaussian, Inc.: Pittsburgh, PA, 1998.

(16) (a) Becke, A. D. *J. Chem. Phys*. **1993**, *98*, 1372. (b) Becke, A. D. *J. Chem. Phys*. **1993**, *98*, 5648.

(17) Cheeseman, J. R.; Frisch, M. J.; Devlin, F. J.; Stephens, P. J. *Chem. Phys. Lett*. **1996**, *252*, 211.

(18) Helgaker, T.; Jensen, H. J. Aa., Joergensen, P., Olsen, J., Ruud, K., Aagren, H.; Auer, A. A.; Bak, K. L.; Bakken, V.; Christiansen, O.; Coriani, S.; Dahle, P.; Dalskov, E. K.; Enevoldsen, T.; Fernandez, B.; Haettig, C.; Hald, K.; Halkier, A.; Heiberg, H.; Hettema, H.; Jonsson, D.; Kirpekar, S.; Kobayashi, R.; Koch, H.; Mikkelsen, K. V.; Norman, P.; Packer, M. J.; Pedersen, T. B.; Ruden, T. A.; Sanchez, A.; Saue, T.; Sauer, S. P. A.; Schimmelpfennig, B.; Sylvester-Hvid, K. O.; Taylor, P. R.; Vahtras, O. *Dalton: A Molecular Electronic Structure Program*, release 1.2; 2001.

(19) Frenz, B. A. Structure Determination Package; *SDP User's Guide*, version 17; Enraf-Nonius: Delft, Holland, December 1984.

(20) North, A. C. T.; Philips, D. C.; Mathews, F. S. *Acta Crystallogr., Sect. A* **1968**, *24*, 351−359.

(21) Sheldrick, G. M.; Kruger, G. M.; Goddard, R. *Acta Crystallogr., Sect. A* **1990**, *46*, 467−473 (*SHELXS-86 Structure Solution Program*).

(22) Sheldrick, G. M. *J. Appl. Crystallogr*. **1993** (*SHELXL-93 Structure Refinement Program*).

(23) Flack, H. D. *Acta Crystallogr., Sect. A* **1983**, *39*, 876−881.

(24) University Chemical Laboratory, Cambridge Crystallographic Data Centre, 12 Union Road, Cambridge CB2 1EZ, U. K.